JOURNAL OF GEOPHYSICAL RESEARCH, VOL. 115, D12203, doi:10.1029/2009JD013385, 2010

On the relationships between lightning frequency and thundercloud parameters of regional precipitation systems

Weixin Xu,[1] Edward J. Zipser,[1] Chuntao Liu,[1] and Haiyan Jiang[2]

Received 16 October 2009; revised 12 January 2010; accepted 2 February 2010; published 19 June 2010.

[1] Seasonal variations on lightning activity of precipitation systems over south China and Taiwan before and after the onset of Mei-Yu have been observed by the lightning imager sensor (LIS) on board the Tropical Rainfall Measuring Mission (TRMM) satellite. Lightning storms before Mei-Yu onset show higher probability of lightning, higher flash rate, and larger radar reflectivity in the mixed-phase region than the Mei-Yu regime. However, the probability of lightning occurrence with the same threshold of maximum radar reflectivity or ice scattering signature is similar for land systems before and during Mei-Yu season. Oceanic systems show slightly lower probability of lightning even with the same thresholds. Relationships between a set of TRMM-observed parameters and LIS lightning frequency are further examined. For lightning systems over land, the total area of radar echo above 35 dBZ has a closer relationship with lightning flash rate at the temperature between −5°C and −15°C than other parameters. Area of lower radar reflectivity at colder temperature, e.g., area of 20 dBZ at −40°C, is also highly correlated with lightning frequency. The highest correlation between area of specific radar reflectivity and lightning frequency is found at lower temperatures when the oceanic lightning systems are examined.

Citation: Xu, W., E. J. Zipser, C. Liu, and H. Jiang (2010), On the relationships between lightning frequency and thundercloud parameters of regional precipitation systems, *J. Geophys. Res.*, *115*, D12203, doi:10.1029/2009JD013385.

1. Introduction

[2] Heavy rainfall and flash floods occur frequently and repeatedly after the onset of East Asian Summer Monsoon over south China and Taiwan [*Ding*, 1992; *Chen*, 2004; *Ding and Chan*, 2005; *Chen et al.*, 2006]. The combination of the moist southwesterly low-level jet and large-scale lifting during "Mei-Yu" (first stage of East Asian Summer Monsoon [*Chen*, 1983; *Tao and Chen*, 1987]) is favorable for active convection and heavy precipitation [*Chen and Yu*, 1988; *Chen et al.*, 2000; *Chen and Li*, 1995; *Chen et al.*, 2005]. However, active Mei-Yu storms have weaker convection and lower lightning flash rate than those during the break time or before Mei-Yu period [*Xu et al.*, 2009]. This study explores and quantifies relationships between lightning frequency and various thunderstorm parameters for this specific region.

[3] Relationships between thundercloud parameters and lightning are based upon the generally accepted noninductive charging (NIC) hypothesis [*Latham et al.*, 2007]. In NIC, it is hypothesized that particle-scale charge separation occurs through rebounding collisions between precipitation-sized ice particles and abundant small ice crystals in the presence of supercooled liquid water [*Takahashi*, 1978; *Saunders et al.*, 1991; *Saunders*, 1993; *MacGorman and Rust*, 1998]. Observations from different weather regimes suggest that robust mixed-phase processes in the mixed-phase region (0°C to −40°C) are necessary to generate storm electrification and initiate lightning [*Stolzenburg et al.*, 1998a; 1998b; *Lang and Rutledge*, 2002; *Atlas and Williams*, 2003; *MacGorman et al.*, 2005]. Electrical charging occurs mainly in the "charging zone" containing graupel/hail, ice crystals, and supercooled liquid droplets. The efficiency of charge transfer depends on the size of the ice crystals and the fall speed of the graupel pellets [*Keith and Saunders*, 1990; *Pereyra et al.*, 2000; *Saunders et al.*, 2006].

[4] The NIC hypothesis has been proven sufficiently robust that ice water content and lightning activity are highly correlated, both on the global scale [*Petersen et al.*, 2005] and regional scale [*Petersen and Rutledge*, 2001; *Gauthier et al.*, 2006]. There are some unexplained departures from this high correlation (land versus ocean), and one of the purposes of this paper was to examine these departures more closely for the East Asia region. *Baker et al.* [1999], *Blyth et al.* [2001], and *Deierling et al.* [2005, 2008] have presented what they termed flux hypothesis which suggests that the lightning frequency is roughly proportional to the product of the downward flux of solid precipitation and the upward mass flux of ice crystals at the top of the charging zone based on computations from lightning models [*Baker et al.*, 1995] and field observations. *Latham et al.* [2004] extended the hypothesis and lightning models to derive a direct rela-

[1]Department of Atmospheric Sciences, University of Utah, Salt Lake City, Utah, USA.
[2]Department of Earth and Environment, Florida International University, Miami, Florida, USA.

0148-0227/10/2009JD013385

tionship between lightning frequency and precipitation rate. In addition, observations also indicate a close link between convective rainfall and lightning, both for individual (or ensemble) storms [*Soula and Chauzy*, 2001; *Seity et al.*, 2001] and for long temporal and large spatial domains [e.g., *Sheridan et al.*, 1997; *Petersen and Rutledge*, 1998; *Soriano et al.*, 2001]. The rain rate-lightning relationship has further been employed to improve the estimation of convective rainfall in specific regions [*Tapia et al.*, 1998; *Grecu et al.*, 2000; *Soriano and De Pablo*, 2003]. More basically, vigorous updrafts are necessary to support the existence of graupel and supercooled liquid droplets in the charging zone. Indeed, strong updrafts have been proposed as a good indicator of lightning [*Zipser and Lutz*, 1994] and the updraft-lightning relationships in specific regimes have further been quantitatively examined [*Lang and Rutledge*, 2002; *Tessendorf et al.*, 2005; *Wiens et al.*, 2005; *Deierling and Petersen*, 2008].

[5] Definable relationships between lightning frequency and thunderstorm parameters, if established quantitatively, can have important applications in estimating or forecasting convective intensity and rainfall via incorporation of lightning data, and vice versa. However, an important unresolved question concerns the variability of the lightning-thundercloud property relationships for different weather regimes. Significant differences exist on thresholds for lightning occurrence between land and oceanic weather systems. For example, even with the same passive microwave brightness temperature or the same vertical profile of radar reflectivity, continental storms are much more likely to produce lightning than oceanic systems [*Toracinta et al.*, 2002; *Cecil et al.*, 2005]. The motivating questions here are: Do differences of thresholds for lightning production exist between different weather regimes in the same location? Do quantified relationships of lightning-thunderstorm parameter, e.g., lightning-radar reflectivity, vary between different weather regimes or land/ocean systems?

[6] It is promising that large samples of lightning measurements are available from satellite-borne devices such as the optical transient detector (OTD) [*Christian and Goodman*, 1992], the Tropical Rainfall Measuring Mission (TRMM) [*Kummerow et al.*, 1998], lightning imaging sensor (LIS) [*Christian*, 1999] and will be from the future geostationary lightning mapper [*Christian*, 2008]. The availability of these high temporal and spatial measurements provides strong motivation for quantifying relationships between satellite-observed lightning frequency and storm properties. The first goal of this paper was to explore relationships between TRMM-observed lightning frequency and thunderstorm parameters over the specific region of south China and Taiwan before and after the onset of Mei-Yu. The second goal was to test the variability of those relationships between the preseason and Mei-Yu season regime, as well as between land and nearby oceanic systems.

[7] The specific objectives of this study include

[8] 1. Quantify the seasonal transition on lightning activity and storm properties of precipitating thunder systems before and after the onset of Mei-Yu.

[9] 2. Determine the thresholds of microwave brightness temperature and radar reflectivity for lightning occurrence within different weather regimes and between land and ocean systems.

[10] 3. Examine relationships between LIS lightning frequency and multiple TRMM-observed thundercloud parameters and their regime-related variability.

[11] 4. Determine temperatures where radar reflectivity parameters such as maximum radar reflectivity and area with high radar reflectivities are most highly correlated with lightning flash rate.

[12] This paper is organized as follows. Section 2 describes the data sets and methodology. Seasonal and intraseasonal transitions on lightning activity and storm properties are presented in section 3.1. Section 3.2 tests the variability of lightning occurrence thresholds, then section 3.3 examines correlations of lightning frequency with different thundercloud parameters, and finally specific temperatures with best correlations in different regimes are presented in section 3.4. A summary and conclusion of the results is given in section 4.

2. Methodology

[13] This study is based on precipitating features (storm scale), using the 11 years long TRMM precipitation feature (PF) database [*Nesbitt et al.*, 2000; *Liu et al.*, 2008]. Lightning data are from observations by the TRMM LIS, while thunderstorm parameters are based on measurements from the TRMM precipitation radar (PR) and microwave imager (TMI).

2.1. Selection of PFs

[14] Usually, the southern China and Taiwan Mei-Yu season onset is between 10 and 15 May [*Chen*, 1983; *Ding and Chan*, 2005]. To avoid inclusion of Mei-Yu days into the preseason, 10 May is selected as the onset date. The Mei-Yu season (10 May to 25 June) is further divided into "Mei-Yu" and "Break" using the same definition as that given by *Xu et al.* [2009], which depends on the existence of defined Mei-Yu rainbands. Pre-Meiyu season includes periods from the beginning of April to days before the onset of Mei-Yu: specifically defined from 1 April to 10 May. The analyzed area is the region where most Mei-Yu rainbands exist [*Xu et al.*, 2009], ranging from 19°N to 29°N and 105°E to 125°E. All the PFs (defined as contiguous PR pixels with near surface rain [*Iguchi et al.*, 2000]) in the designated periods over the key region are selected for investigation. PFs over land are classified into three regimes: Pre-Meiyu, Mei-Yu, and Break, while oceanic features in all periods are combined. All the PFs are grouped into lightning/nonlightning features depending on whether the feature contains any LIS-observed lightning flash. Only lightning features are utilized for constructing the correlation between a specific parameter and lightning frequency. Numbers of samples for different regimes are listed in Table 1.

2.2. Selection of Parameters

[15] PFs include most of the original information of pixel-level measurements from PR, TMI, and LIS in terms of storm parameters or properties. Specific details of parameters available in PF and collocation methods are given by *Liu et al.* [2008]. LIS parameters of a PF selected in this study include total flash counts and lightning flash rate. Parameters from TMI and PR selected for the correlation analysis with lightning frequency include minimum 85 GHz polarization corrected temperature (PCT), minimum 37 GHz

Table 1. Samples of Total Precipitation Features and Lightning Features During Different Periods Over Land and All Periods Combined Over Ocean

Regime Statistics	Pre-Meiyu	Mei-Yu	Break	Ocean
Feature population	8615	7102	7867	12787
Lightning features	753	506	759	534
Total flash count	13107	6190	8108	4457
Features >10 flashes	224	123	195	99
Features >50 flashes	59	27	27	12

PCT, maximum radar reflectivity at specific temperature, convective rain rate, area of radar echo higher than certain values at different temperatures, and retrievals of ice water mass. These parameters are defined as follows:

2.2.1. Lightning Flash Rate

[16] The LIS has an ability to view a 600 × 600 km area of the earth with a spatial resolution of between 3 and 6 km. It can monitor individual storms for lightning activity for a period of 80 or 90 s. Therefore, the total flash counts related to an individual feature record all the lightning flashes occur in the feature during the LIS viewing time. Lightning flash rate is defined to be total flash counts in the feature divided by LIS viewing time.

2.2.2. Minimum 85/37 GHz PCT

[17] The TMI brightness temperatures at 85 and 37 GHz are adjusted into the polarization corrected temperature (PCT) to remove the ambiguity between low brightness temperatures due to ice scattering and due to low surface emissivity. The PCT at 85 GHz defined by *Spencer et al.* [1989] and the one at 37 GHz by *Cecil et al.* [2002] are utilized as following:

$$\mathrm{PCT}_{85\ \mathrm{GHz}} = 1.82T_{85\mathrm{v}} - 0.82T_{85\mathrm{h}}, \text{ and}$$

$$\mathrm{PCT}_{37\ \mathrm{GHz}} = 2.20T_{37\mathrm{v}} - 1.20T_{37\mathrm{h}},$$

where T is the brightness temperature, v and h in the subscripts are vertical and horizontal polarization, respectively. Small precipitation-sized ice particles scatter less of the upwelling radiation at longer wavelength. Compared to 85 GHz PCT, 37 GHz PCT is more sensitive to large ice particles in the precipitating systems than to small ice particles. Thus, low values of minimum PCT at 85 GHz tend to indicate a large ice water path, while low values at 37 GHz tend to indicate that the feature contains larger ice particles.

2.2.3. Maximum Radar Reflectivity and Convective Rain Rate

[18] Radar-based parameters have the advantage of presenting information about hydrometeors at different vertical levels. For example, the maximum height of 30 dBZ echo is an indicator of how high the updraft can loft large supercooled liquid or ice particles [*DeMott and Rutledge*, 1998]. Several studies indicate that the presence of radar echoes above a threshold value of 35–40 dBZ in the mixed-phase region is a good indicator of electrical activity sufficient for lightning [*Dye et al.*, 1989; *Buechler and Goodman*, 1990; *Williams et al.*, 1992; *Petersen et al.*, 1996; *Gremillion and Orville*, 1999]. In this study, the maximum radar reflectivity is calculated between temperatures of 10°C to −60°C with 5°C intervals. Note that the 11 year mean vertical temperature profiles of lightning features (based on National Centers for Environmental Prediction data set) over land during premonsoon, Mei-Yu season, and over ocean during all periods are given in Table 2. The convective rain rate is the mean 2A25 near-surface rain rate [*Iguchi et al.*, 2000] for the convective pixels [*Awaka et al.*, 1998].

2.2.4. Area of Radar Reflectivity

[19] Because the radar reflectivity is proportional to the sixth power of the particle size, high radar echo returns (e.g., >35 dBZ) at cold temperatures indicate the presence of large rimed hydrometeors such as graupel while the smaller ice particles are masked. The presence of smaller ice particles and supercooled cloud liquid water are also important in the process of lightning electrification in the mixed-phase region, but we recognize that radar reflectivity data alone cannot yield specific information on either. So we simply proceed by relating the area of occupied by radar reflectivity larger than specific value between 20 and 45 dBZ at different temperatures (0°C to −60°C) to lightning flash rate in lightning features.

2.2.5. Ice Water Mass

[20] Usually, retrievals of the ice water content from radar reflectivity are based on the regime (storm type)-dependent Z-M relationships. Different Z-M correlations have been summarized to retrieve ice water content of graupel/hail [*Heymsfield and Miller*, 1988; *Yagi and Uyeda*, 1980; *Hauser and Amayenc*, 1986] and ice crystals [*Heymsfield and Palmer*, 1986; *Churchill and Houze*, 1984; *Atlas et al.*, 1995] from different field campaigns. Though the ice water content values estimated from different Z-M relationships may differ from each other significantly, their trends of variation are similar [*Deierling et al.*, 2008]. Here we follow *Petersen et al.* [2005] and roughly estimate ice water mass (IWM) from PR reflectivity using a Z-M relationship based on an exponential size distribution reported by *Black* [1990]:

$$\mathrm{IWM} = 1000\pi\rho_{\mathrm{i}}N_0^{3/7}(5.28\times10^{-18}\mathrm{Z}/270)^{4/7}\mathrm{gm}^{-3},$$

where the constant intercept N_0 is set to be $4\times10^6\ \mathrm{m}^{-4}$. IWM is calculated only in the convective area at −15°C. The bulk ice density of 400 kg/m^3 is selected for this subtropical monsoonal regime.

3. Results

3.1. Seasonal Transition of Lightning Activity and Storm Structure

[21] In the 11 year monthly climatology of the studied region, the frequency of lightning activity peaks (April) leads the rainfall peak (June) by 2 months (Figure 1). With a

Table 2. 11 Year (1998–2008) Climatology of Atmospheric Height at Indicated Temperatures Within Centers of Lightning Features in Preseason and Mei-Yu Season Over Land and Both Season Over Ocean, Separately

Temperature (°C)	0	−5	−10	−15	−20	−25	−30	−35	−40
Pre-Meiyu, height (km)	4.4	5.4	6.3	7.1	7.8	8.6	9.3	10.0	10.6
Mei-Yu, height (km)	5.0	6.0	6.9	7.7	8.5	9.2	9.9	10.6	11.2
Ocean, height (km)	4.8	5.8	6.7	7.5	8.3	9.0	9.7	10.4	11.0

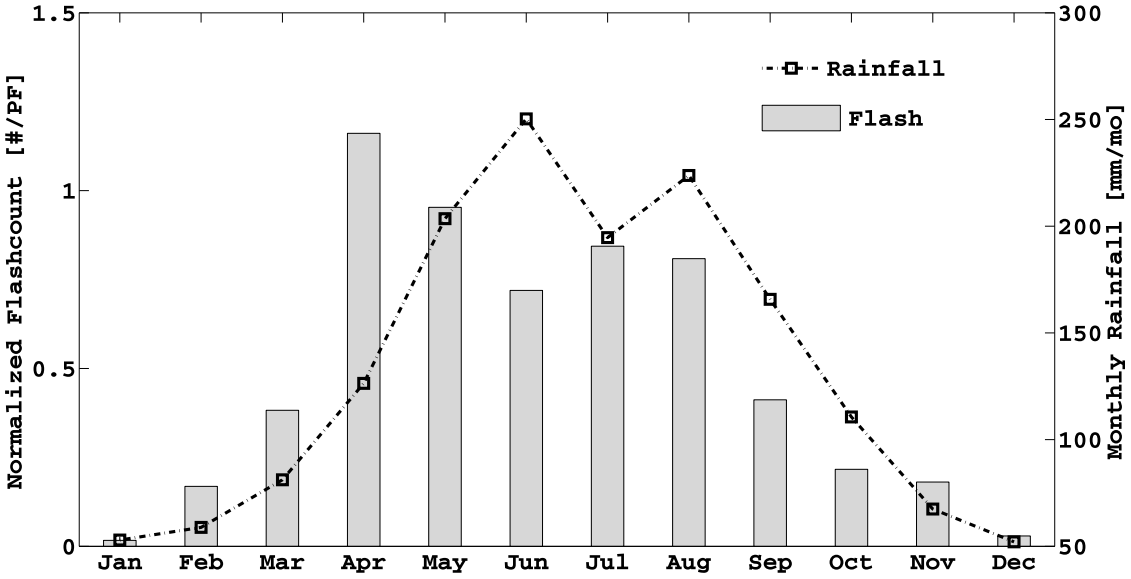

Figure 1. Lightning flash counts normalized by feature population (bar) and 3B42 regional mean monthly rainfall (dash line with square) in the box shown in Figure 2 during 1998–2008.

relative minimum in lightning coinciding with a rainfall peak, this is similar to results for a number of monsoon regimes. For example, *Zipser* [1994] found that the lightning frequency over West Africa has a double peak with the first one leading the rainfall peak, while the thunderstorm minimum accompanies the rainfall peak. Therefore, one might suspect the lightning frequency peak and rainfall maximum to belong to strikingly different regimes, and this proves to be true. Storm properties and convective structures vary significantly from April (preseason) to May–June (Mei-Yu) [*Xu et al.*, 2009]. Table 1 reinforces the fact that a relative minimum in lightning frequency is in phase with active rainfall periods (Mei-Yu), especially over land. For example, during 11 years of pre-Meiyu (440 days) and Mei-Yu periods (180 days), similar numbers of features are found over land, which is 8615 and 7102, respectively. But the number of total lightning flashes in Mei-Yu storms (6190) is less than half of that in the preseason systems (13,107). Lightning features with very high flash rate are twice as frequent in the preseason as those during Mei-Yu. For example, there are more than 50 PFs with lightning flash rate higher than 15 #/min during preseason, but less than 20 PFs reaching that same flash rate during Mei-Yu (Table 1). Not surprisingly, the lowest lightning frequency is found in oceanic storms.

[22] The locations of features with different flash rates before and after the onset of Mei-Yu are shown in Figure 2. Before the onset of Mei-Yu, high flash rate events occur frequently over Indochina Peninsula and spread out over southern to central China. After the onset of Mei-Yu, far less storms with frequent flashes develop, and they stay mostly over southeast foothill of Yun-Gui Plateau in southwestern China and windward side of south China mountain range. This could be the result of orographic initiation and enhancement of the Mei-Yu frontal convection. The low-level warm and moist environment in advance of Mei-Yu fronts also brings more thunderstorms over South China Sea.

[23] The evident seasonal changes on the lightning activity are consistent with variations on the storm structure of lightning systems (Figure 3), although some are fairly subtle. There is no significant difference between Mei-Yu and Break systems, but evident differences exist between pre-Meiyu and Mei-Yu or land and ocean systems. The biggest difference is that pre-meiyu regime has higher radar reflectivity at the level between 0°C and −30°C but lower echo intensity colder than −40°C. This is especially evident for the top 20% lightning features, where the radar echo for the preseason regime is about 3 dBZ higher than in the Mei-Yu season. Some pre-meiyu lightning systems may have hail near the surface (55 dBZ at 1 km). Similar difference on the radar reflectivity structures in the mixed-phase region also exists between land and oceanic lightning features.

3.2. Thresholds for Lightning Occurrence

[24] Thresholds for lightning occurrence in terms of radar reflectivity or microwave brightness temperature in different parts of the world have been examined by many authors [*MacGorman and Rust*, 1998; *Toracinta et al.*, 2002; *Cecil et al.*, 2005; *Yuan and Qie*, 2008]. Their results show that thresholds are land or ocean dependent but very similar in different weather regimes. This study investigates the variability of thresholds for preseason and active monsoon season or land or ocean by examining parameters of maximum radar reflectivity and minimum 85/37 GHz PCT.

[25] Figure 4 shows the probability of lightning occurrence when maximum radar reflectivity at different temperatures reaches specific values. Thresholds required for high probability of lightning occurrence (>60%) are quite close for all the regimes. But for lower probability of lightning (<40%), thresholds vary considerably between land and ocean features. This difference is more evident for systems with lower maximum radar echo at higher temperature, e.g., −5°C or −10°C. It can be concluded that maximum reflectivity of 35 dBZ above −15°C is a good indicator for both land and oceanic regimes in different

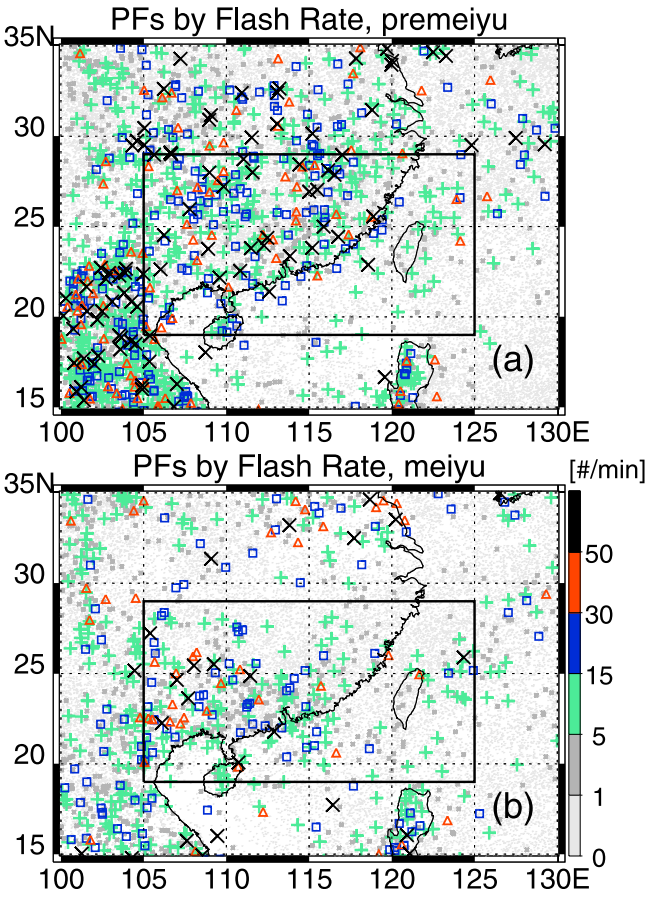

Figure 2. Distribution of precipitation features categorized by lightning flash rate during preseason and Mei-Yu. Values of flash rate (#/min) are indicated by different colors. Markers present features with different flash rate, the values of which are presented according to the colors in the color bar.

weather systems. Radar reflectivity higher than 35 dBZ above the freezing level is suggested to be the requirement of the presence of graupel and supercooled liquid water. But it is interesting that land storms have higher lightning probability than oceanic systems when they have radar reflectivity between 35 and 40 dBZ at temperatures lower than −15°C.

[26] From the perspective of minimum 85 GHz PCT, the probability of lightning occurrence varies significantly among different seasons, and land versus ocean regimes (Figure 5). With the same minimum 85 GHz PCT, the preseason regime tends to have the highest lightning production possibility, while oceanic storms have the least. For example, when minimum 85 GHz PCT is lower than 200 K, more than 80% of the preseason storms produce lightning, while less than 30% of the oceanic features do. However, thresholds of lightning occurrence by minimum PCT get much closer when the frequency shifts to 37 GHz. This is understandable for fact that 85 GHz represents the whole ice water depth, while the depressed 37 GHz PCT indicates larger ice particles (usually in the mixed-phase region). But even for 37 GHz PCT, land systems present much higher probability of lightning when restricted to the same value.

3.3. Correlations Between Lightning and Thundercloud Parameters

[27] Linear correlation coefficients (R) between thunderstorm parameters and lightning flash rate or flash density are presented in Table 3. Scatter diagrams of lightning flash rate versus parameters of minimum 85 GHz PCT, minimum 37 GHz PCT, maximum radar reflectivity near −15°C and area of 35 dBZ echo near −15°C are combined in Figure 6. Linear regression equations for the scatter diagrams in Figure 6 are listed as follows (Y is flash rate, while X is the value of different parameters):

$$(a)\,Y = -0.2306X + 51.4069;\ (b)\,Y = -0.8268X + 221.9749;$$

$$(c)\,Y = 1.6638X - 49.1190;\ \text{and}\ (d)\,Y = 0.018X + 0.6468.$$

The IWM at 8 km is closely correlated (R = 0.80–0.94) with lightning frequency as expected from the literature [*Petersen et al.*, 2005; *Deierling et al.*, 2005; *Latham et al.*, 2007]. Of all the TRMM-observed parameters, 35 dBZ area at −15°C has the best positive relationships (R = 0.78–0.94) with

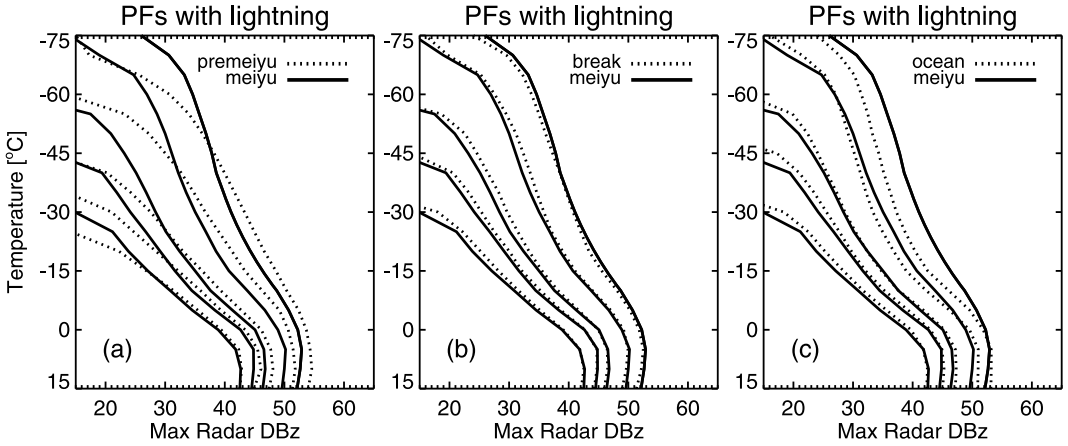

Figure 3. Vertical profile of maximum radar reflectivity for lightning systems during (a) Mei-Yu (solid), before Meiyu (dashed); (b) Mei-Yu (solid), Break (dashed); and (c) Mei-Yu (solid), Ocean (dashed). Ten, 30, 50, 80, and 90 percentile lines are shown.

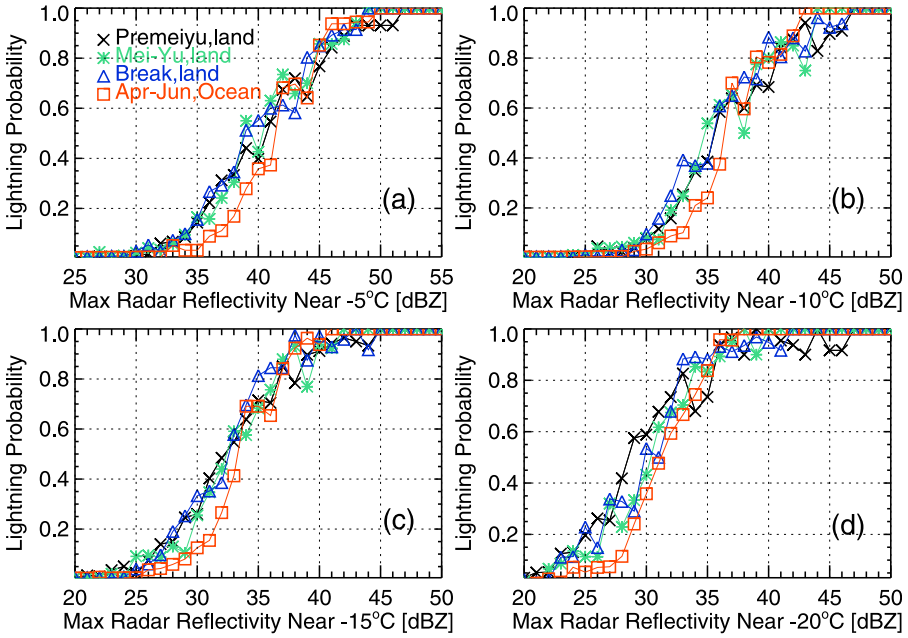

Figure 4. Probability of lightning occurrence within precipitation systems as a function of maximum radar reflectivity near different temperature levels (−5°C, −10°C, −15°C, and 20°C) for land storms during pre-Meiyu (black cross), Mei-Yu (green star), and Break (blue triangle), and Oceanic systems during all periods (red square).

lightning flash rate. This positive linear relation between 35 dBZ area at −15°C and flash rate is extremely good for lightning features with 35 dBZ area larger than 10 pixels (~180 km^2) (Figure 6). This implies that the 35 dBZ area at the mixed-phase region performs as well as the retrieved parameter of IWM as an indicator of precipitation-size ice water and supercooled liquid water content. Similarly, the 20 dBZ area at −40°C also shows very close relationships with lightning frequency (R = 0.76–0.91). Potentially, the 20 dBZ area at upper level of lightning storms could be a good proxy of small nonprecipitation ice content pushed from the mixed-phase region as suggested by *Deierling et al.* [2008]. The correlation between lightning frequency and 35/20 dBZ area is quite consistent within different regimes over land but varies slightly from continental to oceanic regime. For example, continental lightning features have the extremely high correlation (R > 0.90) between flash rate and 35 dBZ area at −15°C while oceanic lightning storms have the lower (R = 0.78).

[28] Although many papers point to a high positive correlation between convective precipitation and lightning [*Soula and Chauzy*, 2001; *Seity et al.*, 2001; *Sheridan et al.*, 1997], it does not show up in this East Asian regime. During the Mei-Yu season, heavy precipitation is frequent but lightning is not. The correlation coefficient between convective rain rate and lightning frequency (R < 0.25) is far lower than that for other parameters in Table 3. This is not a surprise because the relationship between rainfall and lightning is highly regime dependent. Storm electrification by the NIC process requires collisions between graupel and small ice particles in the presence of supercooled cloud liquid water, which in turn requires substantial updrafts in the mixed-phase region. In most tropical ocean regimes, copious rainfall is produced by collision-coalescence low in the cloud, depleting cloud water content before the relatively weak updrafts even reach the mixed-phase region. In contrast, most continental storms not only have stronger updrafts [*Zipser and Lutz*, 1994; *Lucas et al.*, 1994; *Zipser*, 2003] but

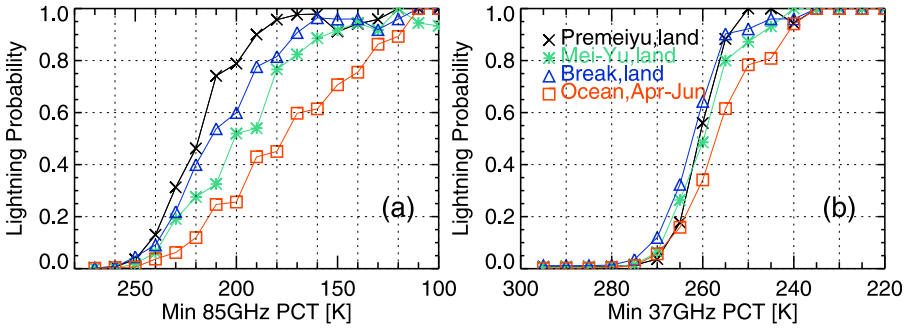

Figure 5. Same as Figure 4 but for the PCT at 85 GHz and 37 GHz.

Table 3. Linear Correlation Coefficients Between Lightning Flash Rate and Indicated Parameters of Lightning Features in Different Periods Over Land and All Periods Combined Over Ocean

Regime Parameter	Pre-Meiyu	Mei-Yu	Break	Ocean
Minimum 85 PCT	−0.51	−0.55	−0.56	−0.45
Minimum 37 PCT	−0.69	−0.70	−0.68	−0.66
Maximum dBZ @ −15°C	0.45	0.53	0.52	0.48
Convective rain rate	0.25	0.18	0.20	0.19
Ice water mass @ −15°C	0.92	0.85	0.87	0.80
35 dBZ area @ −15°C	0.93	0.94	0.90	0.78
20 dBZ area @ −40°C	0.91	0.88	0.87	0.76

also, as *Petersen and Rutledge* [1998] point out, precipitation production is often dominated by processes in the mixed-phase region, so it is logical that the correlation between lightning and convective rain is stronger than over tropical oceans.

[29] The ice scattering signature at both 37 and 85 GHz shows significant negative relationship with lightning frequency (Table 3). In this study, minimum 37 GHz PCT is more highly correlated (R = −0.66 to −0.70) with lightning than minimum 85 GHz PCT (R = −0.45 to −0.56). This is probably related to the fact that 37 GHz PCT depression is due to large ice particles, while 85 GHz PCT is more closely related to the total column ice water content, which may often be due to a large depth of smaller particles. Another speculation is that due to the larger footprint of 37 GHz channel, it may represent those large convective cores better. Maximum radar reflectivity has been used as a good proxy for convection intensity [*Zipser and Lutz*, 1994]. But this pixel proxy presents only moderate relationship with lightning flash rate (R = 0.45–0.53). Pixel proxies including maximum dBZ at 7 km, minimum 85 GHz and 37 GHz PCT represent only the extreme values for a single pixel. But in the real world, the lightning flash count in a large MCS may be contributed by multiple cells or a very large cell with area much larger than one TRMM pixel. Therefore, lightning features with high flash rate (e.g., >20 #/min) show much more scattered relation with pixel proxies than the 35 dBZ echo area proxy (Figure 6).

3.4. Temperature of the Best Correlation and Its Variability

[30] Because the charging zone may involve a temperature range from −5°C to −30°C [*Takahashi*, 1978; *Saunders et al.*, 1991; *Williams et al.*, 1991; *Takahashi and Miyawaki*, 2002], it is of interest to find the temperatures where the best correlation between radar echo and lightning occurs. The 11 year TRMM database can be used to narrow the range of possibilities. The area of radar echo with 35 dBZ at −15°C and 20 dBz at −40°C both show high correlation with lightning frequency. In this section, the correlation coefficients between areas of radar reflectivity with different values at specific temperatures and flash rate are examined (Figure 7). Generally, for continental lightning features, area of high radar reflectivity, e.g., echo >35 dBZ, show their best correlations with lightning frequency at −5°C to −15°C.

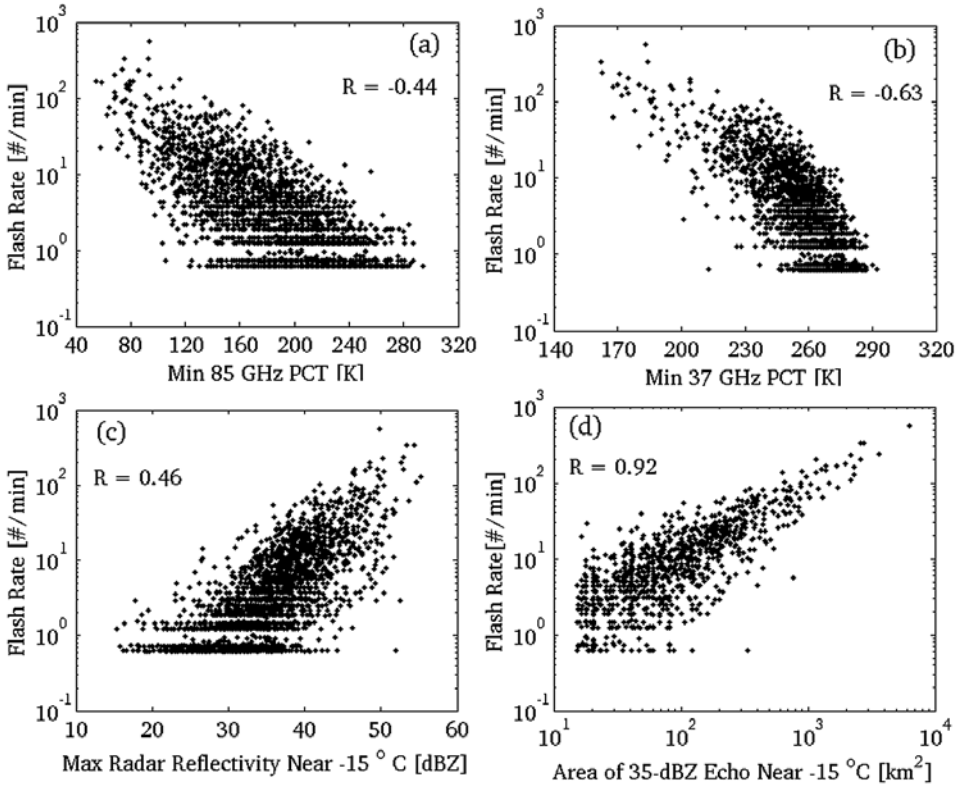

Figure 6. Scatterplot of flash rate versus (a) minimum 85 GHz PCT and (b) minimum 37 GHz PCT, (c) maximum radar reflectivity near −15°C, and (d) area of 35 dBZ echo near −15°C. Character R represents the linear correlation coefficient. Note that Figure 6d only shows the features over land.

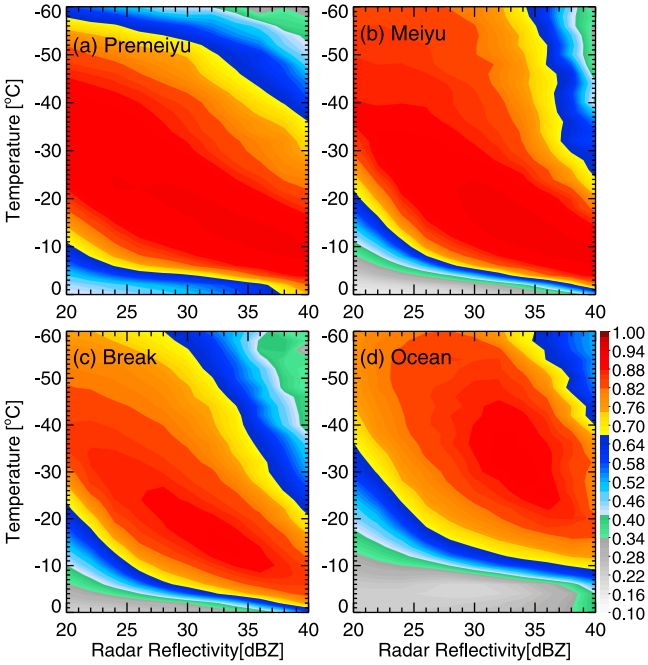

Figure 7. Linear correlation coefficients between lightning flash rate and area of radar reflectivity for land features during (a) pre-meiyu, (b) Mei-Yu, and (c) Break, and (d) for systems in all periods over ocean.

This result agrees with many previous papers and once again supports the NIC hypothesis, directly confirming the altitudes where large hydrometeors are most important. Note that this feature does not vary much with storms over land during different regimes. However, this relationship pattern shifts to lower temperatures for the oceanic lightning systems. Temperatures with highest correlation between high radar reflectivity and flash rate are −15°C to −30°C. Compared to this significant variability between lightning features over land and over ocean, the seasonal variability over land is negligible.

[31] It is interesting that area of 35 dBZ echo at temperatures near −6°C in the oceanic lightning systems is far less correlated (R = 0.26) with lightning flash rate than that of continental lightning features (R = 0.85). This is consistent with the fact that oceanic storms have somewhat lower lightning occurrence than continental features even with the same max radar reflectivity throughout the mixed-phase region (Figure 4). The scatterplot of area of 35 dBZ echo near −6°C versus flash rate shows that any specific lightning flash rate occurs with a wide range of radar reflectivity area over land and an even wider range over ocean (not shown).

[32] Figure 7 indicates that there are good relationships between area of radar reflectivity and lightning flash rate not only in the mixed-phase region but also at colder temperatures. It is understood that charge separation is not expected at such cold temperatures. Usually, large area of high radar reflectivity in the mixed-phase region is accompanied by large area of weaker radar echo at upper levels. It is assumed that small ice particles involved in the charging process may be eventually moved upward and detrained into the anvil region [*Deierling et al.*, 2005; *Deierling et al.*, 2008]. It is true that the stronger the midlevel updraft in the convective core the larger mass of ice particles can be lifted up to higher levels. But, the parameter of 35 dBZ area near −15°C for lightning storms over land and 35 dBZ near −20°C for oceanic lightning features are the most highly correlated with lightning flash rate.

4. Conclusions

[33] TRMM lightning, radar, and microwave measurements are used to investigate the lightning activity before and after the onset of Mei-Yu over southern China, Taiwan, and adjacent ocean. The correlations between a set of thundercloud parameters and lightning frequency, as well as their seasonal and land or ocean variability are examined. The major findings include

[34] 1. Evident seasonal and land/ocean variations exist on lightning frequency, storm structure, and lightning distribution pattern of storms over the study region.

[35] 2. The thresholds for lightning occurrence vary significantly only between continental and oceanic regimes at the temperature below −15°C. With the same maximum radar reflectivity lower than 35 dBZ at temperature such as −10°C, continental storms have higher probability of lightning than their oceanic counterparts. Similarly, with the same minimum brightness temperature at 37 or 85 GHz, continental storms have higher probability of lightning than their oceanic counterparts.

[36] 3. Of all the examined parameters, area of 35 dBZ in the mixed-phase region, as well as roughly estimated ice water mass at midlevel, are best correlated with lightning flash rate.

[37] 4. Temperatures of maximum correlation between area of specific radar reflectivity and flash rate differ considerably between land and oceanic lightning storms. The area of high radar reflectivity, e.g., 35 dBZ, has its highest correlation with lightning frequency at −5°C to −15°C over land but at −15°C to −30°C over ocean.

[38] These results continue to beg the question of why the lightning probability or flash rate can be lower over oceans than over land for very similar measured values of microwave brightness temperature or radar reflectivity. Rather than speculate with little evidence, we defer this issue to future papers. However, we do point out the following points. Other things being equal, updrafts over land are likely to have higher supercooled liquid water contents than over ocean, where cloud water is converted to rain more quickly and depletes cloud water more efficiently before the updraft reaches the mixed-phase region. Also, the greatest difference between land and ocean in Figure 7 is in the temperature range of −5°C to −8°C (~6 km), above which oceanic clouds often have a very rapid decrease in reflectivity with altitude compared with continental clouds [*Zipser and Lutz*, 1994; *Liu et al.*, 2008], so it is possible that many of the oceanic (land) systems with large areas of 35 dBZ echo at −6°C have smaller (larger) area of 35 dBZ at −10°C to −15°C where charge separation is more likely.

[39] This study not only adds details to the knowledge of the behavior of weather systems in the East Asian summer monsoon region but also provides clues to a broader context. First, it presents important fundamental knowledge of the relationships between TRMM-observed quantities and LIS-measured lightning. Second, thresholds of lightning occur-

rence and correlation between lightning and thundercloud parameters between land and oceanic regimes vary strikingly but stay quite stable over land among preseason, Mei-Yu, and Break period. This warrants the examination of lightning probability and lightning-storm property relationship on the different meteorological regimes globally in the future.

[40] **Acknowledgments.** The comments of the three anonymous reviewers were very helpful in improving the manuscript. This research was supported by NASA Precipitation Measurement Mission grant NAG5-13628 under the direction of Ramesh Kakar. Special thanks are given to the TRMM Science Data and Information System group led by Erich Stocker and John Kwiatkowski at NASA Goddard Space Flight Center, Greenbelt, Maryland, for data processing assistance.

References

Atlas, D., and C. R. Williams (2003), The anatomy of a continental convective storm, *J. Atmos. Sci.*, *60*, 3–15, doi:10.1175/1520-0469(2003)060<0003:TAOACT>2.0.CO;2.

Atlas, D., S. Y. Matrosov, A. J. Heymsfield, M.-D. Chou, and D. B. Wolff (1995), Radar and radiation properties of ice clouds, *J. Appl. Meteorol.*, *34*, 2329–2345, doi:10.1175/1520-0450(1995)034<2329:RARPOI>2.0.CO;2.

Awaka, J., T. Iguchi, and K. Okamoto (1998), Rain type classification algorithm, *Space*, *3*, 213–224.

Baker, M. B., H. J. Christian, and J. Latham (1995), A computational study of the relationships linking lightning frequency and other thundercloud parameters, *Q. J. R. Meteorol. Soc.*, *121*, 1525–1548, doi:10.1002/qj.49712152703.

Baker, M. B., A. M. Blyth, H. J. Christian, J. Latham, K. L. Miller, and A. M. Gadian (1999), Relationships between lightning activity and various thundercloud parameters: Satellite and modelling studies, *Atmos. Res.*, *51*, 221–236, doi:10.1016/S0169-8095(99)00009-5.

Black, R. A. (1990), Radar reflectivity-ice water content relationships for use above the melting level in hurricanes, *J. Appl. Meteorol.*, *29*, 955–961, doi:10.1175/1520-0450(1990)029<0955:RRIWCR>2.0.CO;2.

Blyth, A. M., H. J. Christian, K. Driscoll, A. Gadian, and J. Latham (2001), Determination of ice precipitation rates and thunderstorm anvil ice contents from satellite observations of lightning, *Atmos. Res.*, *59–60*, 217–229, doi:10.1016/S0169-8095(01)00117-X.

Buechler, D. E., and S. J. Goodman (1990), Echo size and asymmetry: Impact on NEXRAD storm identification, *J. Appl. Meteorol.*, *29*, 962–969, doi:10.1175/1520-0450(1990)029<0962:ESAAIO>2.0.CO;2.

Cecil, D. J., E. J. Zipser, and S. W. Nesbitt (2002), Reflectivity, ice scattering, and lightning characteristics of hurricane eye walls and rainbands. Part I: Quantitative description, *Mon. Weather Rev.*, *130*, 769–784, doi:10.1175/1520-0493(2002)130<0769:RISALC>2.0.CO;2.

Cecil, D. J., S. J. Goodman, and D. J. Boccippio (2005), Three years of TRMM precipitation features. Part I: Radar, radiometric, and lightning characteristics, *Mon. Weather Rev.*, *133*, 543–566, doi:10.1175/MWR-2876.1.

Chen, G. T.-J. (1983), Observational aspects of the Meiyu phenomena in subtropical China, *J. Meteorol. Soc. Jpn.*, *61*, 306–312.

Chen, G. T.-J. (2004), Research on the phenomena of Meiyu during the past quarter century: An overview, in *The East Asian Monsoon*, edited by C.-P. Chang, pp. 357–403, World Sci., Hackensack, N.J.

Chen, G. T.-J., and C.-C. Yu (1988), Study of low-level jet and extremely heavy rainfall over northern Taiwan in the Mei-Yu season, *Mon. Weather Rev.*, *116*, 884–891, doi:10.1175/1520-0493(1988)116<0884:SOLLJA>2.0.CO;2.

Chen, G. T.-J., C.-C. Wang, and D. T.-W. Lin (2005), Characteristics of low-level jets over northern Taiwan in Mei-Yu season and their relationship to heavy rain events, *Mon. Weather Rev.*, *133*, 20–43, doi:10.1175/MWR-2813.1.

Chen, G. T.-J., C.-C. Wang, and L.-F. Lin (2006), A diagnostic study of a retreating Mei-Yu front and the accompanying low-level jet formation and intensification, *Mon. Weather Rev.*, *134*, 874–896, doi:10.1175/MWR3099.1.

Chen, S.-J., W. Wang, K. H. Lau, Q. H. Zhang, and Y. S. Chung (2000), Mesoscale convective systems along the Meiyu front in a numerical model, *Meteorol. Atmos. Phys.*, *75*, 149–160, doi:10.1007/s007030070002.

Chen, Y.-L., and J. Li (1995), Large-scale conditions favorable for the development of heavy rainfall during TAMEX IOP 3, *Mon. Weather Rev.*, *123*, 2978–3002, doi:10.1175/1520-0493(1995)123<2978:LSCFFT>2.0.CO;2.

Christian, H. J. (1999), Optical detection of lightning from space, paper presented at International Conference on Atmospheric Electricity, *NASA/CP-1999–209261*, pp. 715–718, Guntersville, Ala, 10–11 June.

Christian, H. J., Jr. (2008), The Geostationary lightning mapper instrument for GOES-R, in *AMS 88th Annual Meeting*, New Orleans, La, U.S.A., 20–24 January.

Christian, H. J., and S. Goodman (1992), Global observations of lightning from space, in *Proc. 9th Internat. Conf. on Atmos. Electr.*, pp. 316–321, St. Petersburg.

Churchill, D. D., and R. A. Houze Jr. (1984), Mesoscale updraft magnitude and cloud-ice content deduced from the ice budget of the stratiform region of a tropical cloud cluster, *J. Atmos. Sci.*, *41*, 1717–1725, doi:10.1175/1520-0469(1984)041<1717:MUMACI>2.0.CO;2.

Deierling, W., and W. A. Petersen (2008), Total lightning activity as an indicator of updraft characteristics, *J. Geophys. Res.*, *113*(D16), D16210, doi:10.1029/2007JD009598.

Deierling, W., J. Latham, W. A. Petersen, S. M. Ellis, and H. J. Christian Jr. (2005), On the relationship of thunderstorm ice hydrometeor characteristics and total lightning measurements, *Atmos. Res.*, *76*, 114–126, doi:10.1016/j.atmosres.2004.11.023.

Deierling, W., W. A. Petersen, J. Latham, S. Ellis, and H. J. Christian (2008), The relationship between lightning activity and ice fluxes in thunderstorms, *J. Geophys. Res.*, *113*(D15), D15210, doi:10.1029/2007JD009700.

DeMott, C. A., and S. A. Rutledge (1998), The vertical structure of TOGA COARE convection. Part I: Radar echo distributions, *J. Atmos. Sci.*, *55*, 2730–2747, doi:10.1175/1520-0469(1998)055<2730:TVSOTC>2.0.CO;2.

Ding, Y. (1992), Summer monsoon rainfalls in China, *J. Meteorol. Soc. Jpn.*, *70*, 373–396.

Ding, Y., and J. C.-L. Chan (2005), The East Asian summer monsoon: An overview, *Meteorol. Atmos. Phys.*, *89*, 117–142, doi:10.1007/s00703-005-0125-z.

Dye, J. E., W. P. Winn, J. J. Jones, and D. W. Breed (1989), The electrification of New Mexico thunderstorms. 1. Relationship between precipitation development and the onset of electrification, *J. Geophys. Res.*, *94*, 8643–8656, doi:10.1029/JD094iD06p08643.

Gauthier, M. L., W. A. Petersen, L. D. Carey, and H. J. Christian Jr. (2006), Relationship between cloud-to-ground lightning and precipitation ice mass: A radar study over Houston, *Geophys. Res. Lett.*, *33*, L20803, doi:10.1029/2006GL027244.

Grecu, M., E. N. Anagnostou, and R. F. Adler (2000), Assessment of the use of lightning information in satellite Infrared rainfall estimation, *J. Hydrometeorol.*, *1*, 211–221, doi:10.1175/1525-7541(2000)001<0211:AOTUOL>2.0.CO;2.

Gremillion, M. S., and R. E. Orville (1999), Thunderstorm characteristics of cloud-to-ground lightning at the Kennedy Space Center, Florida: A study of lightning initiation signatures as indicated by the WSR-88D, *Weather Forecast.*, *14*, 640–649, doi:10.1175/1520-0434(1999)014<0640:TCOCTG>2.0.CO;2.

Hauser, D., and P. Amayenc (1986), Retrieval of cloud water and water vapor contents from Doppler radar data in a tropical squall line, *J. Atmos. Sci.*, *43*, 823–838, doi:10.1175/1520-0469(1986)043<0823:ROCWAW>2.0.CO;2.

Heymsfield, A. J., and K. M. Miller (1988), Water vapor and ice mass transported into the anvils of CCOPE thunderstorms: Comparison with storm influx and rainout, *J. Atmos. Sci.*, *45*, 3501–3514, doi:10.1175/1520-0469(1988)045<3501:WVAIMT>2.0.CO;2.

Heymsfield, A. J., and A. G. Palmer (1986), Relations for deriving thunderstorm anvil mass of CCOPE storm water budget estimates, *J. Clim. Appl. Meteorol.*, *25*, 691–702, doi:10.1175/1520-0450(1986)025<0691:RFDTAI>2.0.CO;2.

Iguchi, T., T. Kozu, R. Meneghini, J. Awaka, and K. Okamoto (2000), Rain-profiling algorithm for the TRMM precipitation radar, *J. Appl. Meteorol.*, *39*, 2038–2052, doi:10.1175/1520-0450(2001)040<2038:RPAFTT>2.0.CO;2.

Keith, W. D., and C. P. R. Saunders (1990), Further laboratory studies of the charging of graupel during ice crystal interactions, *Atmos. Res.*, *25*, 445–464, doi:10.1016/0169-8095(90)90028-B.

Kummerow, C., W. Barnes, T. Kozu, J. Shiue, and J. Simpson (1998), The Tropical Rainfall Measuring Mission (TRMM) sensor package, *J. Atmos. Oceanic Technol.*, *15*, 809–817, doi:10.1175/1520-0426(1998)015<0809:TTRMMT>2.0.CO;2.

Lang, T. J., and S. A. Rutledge (2002), Relationship between convective storm kinematics, precipitation, and lightning, *Mon. Weather Rev.*, *130*, 2492–2506, doi:10.1175/1520-0493(2002)130<2492:RBCSKP>2.0.CO;2.

Latham, J., A. M. Blyth, H. J. Christian Jr., W. Deierling, and A. M. Gadian (2004), Determination of precipitation rates and yields from lightning measurements, *J. Hydrol. Amsterdam*, *288*, 13–19, doi:10.1016/j.jhydrol.2003.11.009.

Latham, J., W. A. Petersen, W. Deierling, and H. J. Christian (2007), Field identification of a unique globally dominant mechanism of thunderstorm electrification, *Q. J. R. Meteorol. Soc.*, *133*, 1453–1457.

Liu, C., E. J. Zipser, D. J. Cecil, S. W. Nesbitt, and S. Sherwood (2008), A cloud and precipitation feature database from nine years of TRMM observations, *J. Appl. Meteorol.*, *47*, 2712–2728, doi:10.1175/2008JAMC1890.1.

Lucas, C., E. J. Zipser, and M. A. Lemone (1994), Vertial velocity in oceanic convection off tropical Australia, *J. Atmos. Sci.*, *51*, 3181–3193, doi:10.1175/1520-0469(1994)051<3183:VVIOCO>2.0.CO;2.

MacGorman, D. R., and W. D. Rust (1998), *The Electrical Nature of Storms*, 422 pp., Oxford Univ. Press, New York.

MacGorman, D. R., W. D. Rust, P. Krehbiel, W. Rison, E. Bruning, and K. Wiens (2005), The electrical structure of two supercell storms during STEPS, *Mon. Weather Rev.*, *133*, 2583–2607, doi:10.1175/MWR2994.1.

Nesbitt, S. W., E. J. Zipser, and D. J. Cecil (2000), A census of precipitation features in the tropics using TRMM: Radar, ice scattering, and lightning observations, *J. Clim.*, *13*, 4087–4106, doi:10.1175/1520-0442(2000)013<4087:ACOPFI>2.0.CO;2.

Pereyra, R. G., E. E. Avila, N. E. Castellano, and C. Saunders (2000), A laboratory study of graupel charging, *J. Geophys. Res.*, *105*(D16), 20,803–20,812, doi:10.1029/2000JD900244.

Petersen, W. A., and S. A. Rutledge (1998), On the relationship between cloud-to-ground lightning and convective rainfall, *J. Geophys. Res.*, *103*, 14,025–14,040, doi:10.1029/97JD02064.

Petersen, W. A., and S. A. Rutledge (2001), Regional variability in tropical convection: Observations from TRMM, *J. Clim.*, *14*, 3566–3586, doi:10.1175/1520-0442(2001)014<3566:RVITCO>2.0.CO;2.

Petersen, W. A., S. A. Rutledge, and R. E. Orville (1996), Cloud-to-ground lightning observations from TOGA COARE: Selected results and lightning location algorithms, *Mon. Weather Rev.*, *124*, 602–620, doi:10.1175/1520-0493(1996)124<0602:CTGLOF>2.0.CO;2.

Petersen, W. A., H. J. Christian, and S. A. Rutledge (2005), TRMM observations of the global relationship between ice water content and lightning, *Geophys. Res. Lett.*, *32*, L14819, doi:10.1029/2005GL023236.

Saunders, C. P. R. (1993), A review of the thunderstorm electrification processes, *J. Appl. Meteorol.*, *32*, 642–655, doi:10.1175/1520-0450(1993)032<0642:AROTEP>2.0.CO;2.

Saunders, C. P. R., W. D. Keith, and R. P. Mitzeva (1991), The effect of liquid water on thunderstorm charging, *J. Geophys. Res.*, *96*(D6), 11,007–11,017, doi:10.1029/91JD00970.

Saunders, C. P. R., H. Bax-Norman, C. Emersic, E. E. Avila, and N. E. Castellano (2006), Laboratory studies of the effect of cloud conditions on graupel/crystal charge transfer in thunderstorm electrification, *Q. J. R. Meteorol. Soc.*, *132*, 2653–2673, doi:10.1256/qj.05.218.

Seity, Y., S. Soula, and H. Sauvageot (2001), Lightning and precipitation activities in coast thunderstorms, *J. Geophys. Res.*, *106*(D19), 22,801–22,816, doi:10.1029/2001JD900244.

Sheridan, S. C., J. F. Griffiths, and R. E. Orville (1997), Warm season cloud-to-ground lightning-precipitation relationships in the south-central United states, *Weather Forecast.*, *12*, 449–458, doi:10.1175/1520-0434(1997)012<0449:WSCTGL>2.0.CO;2.

Soriano, L. R., and F. De Pablo (2003), Analysis of convective precipitation in the western Mediterranean Sea through the use of cloud-to-ground lightning, *Atmos. Res.*, *66*, 189–202, doi:10.1016/S0169-8095(02)00160-6.

Soriano, L. R., F. De Pablo, and E. G. Diez (2001), Relationship between convective precipitation and cloud-to-ground lightning in the Iberian peninsula, *Mon. Weather Rev.*, *129*, 2998–3003, doi:10.1175/1520-0493(2001)129<2998:RBCPAC>2.0.CO;2.

Soula, S., and S. Chauzy (2001), Some aspects of the correlation between lightning and rain activities in severe storms, *Atmos. Res.*, *56*, 355–373, doi:10.1016/S0169-8095(00)00086-7.

Spencer, R. W., H. G. Goodman, and R. E. Hood (1989), Precipitation retrieval over land and ocean with the SSM/I: Identification and characteristics of the scattering signal, *J. Atmos. Oceanic Technol.*, *6*, 254–273, doi:10.1175/1520-0426(1989)006<0254:PROLAO>2.0.CO;2.

Stolzenburg, M., W. D. Rust, B. F. Smull, and T. C. Marshall (1998a), Electrical structure in thunderstorm convective regions 1. Mesoscale convective systems, *J. Geophys. Res.*, *103*(D12), 14,059–14,078, doi:10.1029/97JD03546.

Stolzenburg, M., W. D. Rust, and T. C. Marshall (1998b), Electrical structure in thunderstorm convective regions: 2. Isolated storms, *J. Geophys. Res.*, *103*, 14,097–14,096, doi:10.1029/97JD03545.

Takahashi, T. (1978), Riming electrification as a charge generation mechanism in thunderstorms, *J. Atmos. Sci.*, *35*, 1536–1548, doi:10.1175/1520-0469(1978)035<1536:REAACG>2.0.CO;2.

Takahashi, T., and K. Miyawaki (2002), Reexamination of rimming of electrification in a wind tunnel, *J. Atmos. Sci.*, *59*, 1018–1025, doi:10.1175/1520-0469(2002)059<1018:ROREIA>2.0.CO;2.

Tao, S., and L. Chen (1987), A review of recent research on the East Asian summer monsoon in China, in *Monsoon Meteorology*, edited by C.-P. Change and T. N. Krishnamurti, pp. 60–92, Oxford Univ. Press, U.S.A.

Tapia, A., J. Smith, and M. Dixon (1998), Estimation of convective rainfall from lightning observations, *J. App. Met.*, *37*, 1497–1509, doi:10.1175/1520-0450(1998)037<1497:EOCRFL>2.0.CO;2.

Tessendorf, S. A., L. J. Miller, K. C. Wiens, and S. A. Rutledge (2005), The 29 June 2000 supercell observed during STEPS. Part I: Kinematics and microphysics, *J. Atmos. Sci.*, *62*, 4127–4150, doi:10.1175/JAS3585.1.

Toracinta, R., D. J. Cecil, E. J. Zipser, and S. W. Nesbitt (2002), Radar, passive microwave, and lightning characteristics of precipitating systems in the tropics, *Mon. Weather Rev.*, *130*, 802–823, doi:10.1175/1520-0493(2002)130<0802:RPMALC>2.0.CO;2.

Wiens, K. C., S. A. Rutledge, and S. A. Tessendorf (2005), The 29 June 2000 supercell observed during STEPS. Part II: Lightning and charge structure, *J. Atmos. Sci.*, *62*, 4151–4177, doi:10.1175/JAS3615.1.

Williams, E. R., R. Zhang, and J. Rydock (1991), Mixed-phase microphysics and cloud electrification, *J. Atmos. Sci.*, *48*, 2195–2203, doi:10.1175/1520-0469(1991)048<2195:MPMACE>2.0.CO;2.

Williams, E. R., S. A. Rutledge, S. G. Geotis, N. Renno, E. Rasmussen, and T. Rickenbach (1992), A radar and electrical study of tropical "hot towers", *J. Atmos. Sci.*, *49*, 1386–1395, doi:10.1175/1520-0469(1992)049<1386:ARAESO>2.0.CO;2.

Xu, W., E. J. Zipser, and C. Liu (2009), Rainfall characteristics and convective properties of Mei-Yu precipitation systems over south China and Taiwan, Part I: TRMM observations, *Mon. Weather Rev.*, *137*, 4261–4275, doi:10.1175/2009MWR2982.1.

Yagi, T., and H. Uyeda (1980), Different size distributions of snow based on meteorological situations, in *Communications a la VIIIeme Conference International sur la Physique des Nuages*, pp. 231–234, ClermontFerrand, France.

Yuan, T., and X. Qie (2008), Study on lightning activity and precipitation characteristics before and after the onset of the South China Sea summer monsoon, *J. Geophys. Res.*, *113*, D14101, doi:10.1029/2007JD009382.

Zipser, E. J. (1994), Deep cumulonimbus cloud systems in the tropics with and without lightning, *Mon. Weather Rev.*, *122*, 1837–1851, doi:10.1175/1520-0493(1994)122<1837:DCCSIT>2.0.CO;2.

Zipser, E. J. (2003), Some view on "hot tower" after 50 years of tropical field programs and two years of TRMM data, in *Cloud Systems, Hurricanes, and the Tropical Rainfall Measuring Mission (TRMM)*, edited by W.-K. Tao and R. Adler, *Meteorol. Monogr., 29*, 49–58.

Zipser, E. J., and K. R. Lutz (1994), The vertical profile of radar reflectivity of convective cells: A strong indicator of storm intensity and lightning probability, *Mon. Weather Rev.*, *122*, 1751–1759, doi:10.1175/1520-0493(1994)122<1751:TVPORR>2.0.CO;2.

H. Jiang, Department of Earth and Environment, Florida International University, 11200 SW 8th Street, PC-342B, Miami, FL 33199, USA.

C. Liu, W. Xu, and E. J. Zipser, Department of Atmospheric Sciences, Meteorology, University of Utah, 135 S 1460 East, Rm. 819, Salt Lake City, UT 84112-0110, USA. (weixin.xu@utah.edu)